IEEE Access
The journal for rapid open access publishing

Received October 4, 2015, accepted October 17, 2015, date of publication October 30, 2015, date of current version November 5, 2015.

Digital Object Identifier 10.1109/ACCESS.2015.2495226

Dynamic Scheduling for High Throughput Satellites Employing Priority Code Scheme

LILIAN DEL CONSUELO HERNANDEZ RUIZ GAYTAN[1], (Member, IEEE), ZHENNI PAN[2], (Member, IEEE), JIANG LIU[3], (Member, IEEE), AND SHIGERU SHIMAMOTO[2], (Member, IEEE)

[1]Graduate School of Global Information and Telecommunication Studies, Waseda University, Tokyo 169-0072, Japan
[2]Department of Communications and Computer Engineering, Waseda University, Tokyo 169-0072, Japan
[3]International Center for Science and Engineering Programs, Faculty of Science and Engineering, Waseda University, Tokyo 169-0072, Japan

Corresponding author: L. del Consuelo Hernandez Ruiz Gaytan (lilianhrg@gmail.com)

This work was supported by the Ministry of Education, Culture, Sports, Science and Technology of Japan under Grant 1570061503.

ABSTRACT Based on the use of multi-beams, high throughput satellites (HTSs) provide high data rates to a large number of users. In this context, the distribution of frequency resources among multi-beams plays an important role. This is because unsuitable distributions might cause the wastage or the starvation of frequencies and bring about low throughput rates. This paper proposes a solution to mitigate the unsuitable allocations of frequency resources in an HTS. The solution is the priority code scheme (PCS), which seeks to respond to users' demands by dynamically scheduling frequency resources for precise satellite footprint areas. The key is to assign a priority code and an efficiency indicator to every multi-beam deployed on the system. The PCS algorithm involves the association of the efficiency indicator with the bandwidth utilization per beam to detect and correct arbitrary bandwidth allocations among the beams. Due to the PCS's cyclical repetition of its algorithm, the concurrence time of the scheme and the tardiness of the algorithm form part of the evaluation of the PCS. Furthermore, we support the implementation of the frequency-reuse process to enhance the exploitation of frequency resources. To evaluate the PCS performance, the analysis delves into the study of the bandwidth utilization, the interference among beams, the concurrence time, and the algorithm tardiness.

INDEX TERMS Algorithm, bandwidth allocation, high throughput satellites, interference, multi-beams, priority codes, and scheduling.

I. INTRODUCTION

A. BACKGROUND

In terms of cost/benefit contributions, increasing the satellite's throughput makes the satellite technology relevant for future communication systems. To satisfy the incoming network requirements, increasing the transmission power level enriches the system's bandwidth. However, the benefits are not sufficient for supporting services with high throughput demands. High Throughput Satellites (HTS) [1]–[5] have proven to represent affordable solutions that provide high data rates to a large number of users. Based on the application of the multi-beam technique [6], HTS improves the bandwidth management reaching instantaneous data rates of up to 100 Gbps. Although dynamic user demands remain unsatisfied, the beam hopping technique [7] renders the system more flexible than the non-beam-hopped system. In addition, the combination of switching and beam hopping techniques translates into an interesting analysis [8], making it possible to reach the targeted capacity in geostationary (GEO) satellite networks. To perform a frequency resource allocation in Spatial Division Multiple Access (SDMA) satellite systems, the beam moving technique [9] involves continuous adjustment of satellite beams and offers the advantage of dealing with non-linear changes of interference. On the other hand, the frequency resource allocation, that is based on finding the Maximum Weight Independent Set (MWIS) [10] in a weighted interference graph of each single channel, shows a promising allocation technique. However, the inter-beam interference represents a critical factor to attend to.

B. PROBLEM

The authors' concern is that previous studies do not include one of the main problems that several mobile communication systems face and that is the unsuitable allocation

of frequency resources. The concern is based on the evidence that the schedulers currently employed assign frequency resources once at the beginning of the algorithm but do not adjust the resource assignation later, when the user needs have changed. That means that the current schemes assign fixed bandwidth allocations to each beam in the system, assuming that the users served by those beams have constant needs. However, real users, in accordance with the incoming necessities, adopt different behaviors from time to time requiring a particular quantity of frequency resources at a particular moment and another quantity a few seconds or minutes later. As a result of assuming that users have static behaviors, current schemes succeed in employing a practical method that is easy to handle. At the same time, current schemes fail by performing frequency resource allocations that tend to be unsatisfactory and arbitrary among the massive number of final users. This causes either of two undesirable scenarios: 1) the wastage of allocated frequency resources due to the lack of service requests, defined as the overload bandwidth scenario, and 2) the rejection of service requests due to the lack of frequency resources, defined as the underload bandwidth scenario. Inadequate frequency resource allocation has various effects on the satellite systems, for instance, low throughput, the abortion of current tasks, and the rejection of incoming requirements. Therefore, for the efficient management of frequency resources, the reduction of deficient bandwidth allocations among the multi-beams is indispensable. In order to improve the bandwidth allocation process, the creation of new schemes is necessary.

C. PROPOSAL

The authors propose a novel scheme named the priority code scheme (PCS) [12]. The basic principle of the PCS is to execute a dynamic bandwidth allocation in accordance with several factors, namely, the user's frequency demands, the unallocated frequency resources, the efficiency ratio, and the efficiency threshold associated with each beam. The efficiency threshold identifies two undesirable scenarios: 1) the overload bandwidth scenario and 2) the underload bandwidth scenario. Therefore, the PCS is a useful alternative to performing bandwidth allocations in realistic environments where the users' needs change constantly. Hence, the scheme description explains the importance of the PCS. Although the authors of the present paper previously introduced the PCS concept [12], including the PCS's basic principle, they excluded the analysis of the concurrence time and the algorithm tardiness of the scheme. The concurrence time defines how periodically the PCS should run its algorithm. The algorithm tardiness refers to the speed at which the PCS runs its algorithm. Due to the PCS's cyclical repetition of its algorithm, the evaluation of the concurrence time and the algorithm tardiness are crucial confirmations. Therefore, the analysis of both parameters consitutes part of the present paper. The authors also intend to improve the original PCS design [12] by considering the frequency-resource process in the analysis. Fig. 1 illustrates the PCS system model, whereas

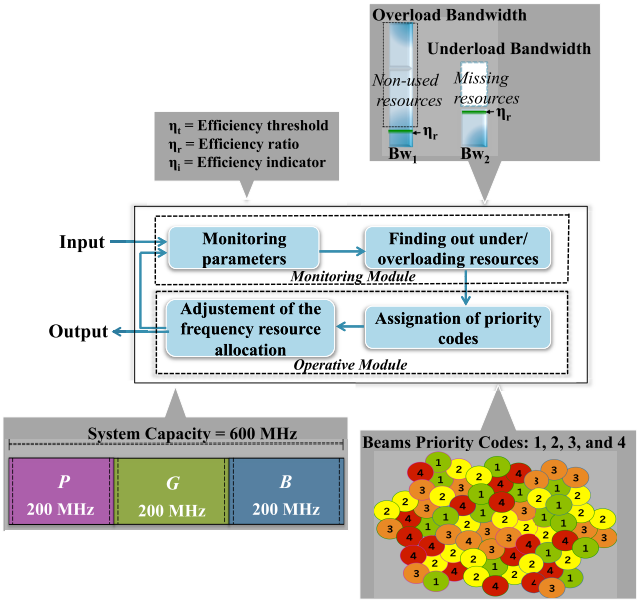

FIGURE 1. PCS system model.

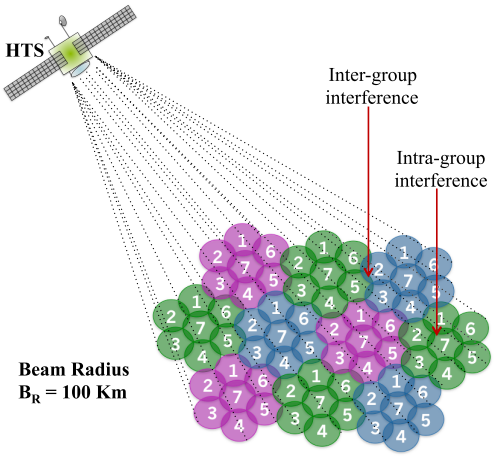

FIGURE 2. PCS frequency-reuse pattern.

Fig. 2 represents an image of the PCS frequency-reuse pattern of 70 beams in the HTS in GEO orbit. The frequency-reuse process might enhance the use of frequency resources. Furthermore, it might increase the inter/intra-beam group interference among the multi-beams in the system. Consequently, the authors have undertaken a deeper analysis of the PCS, considering the additional alternatives and their associated risks. To facilitate the understanding of the present paper, in the following sections, the authors carefully distinguish between the PCS's basic principle and the corresponding results, which are the merits of previous works [12], and the new PCS characteristics and methods, which are the merits of the present paper. The authors expect to add reliability to the PCS with the results that the present research offers.

The remainder of this paper is organized in four sections. Section II briefly describes the principle of the PCS. Section III introduces the PCS's additional challenges and describes the problems involved. Section IV presents the

evaluation of the PCS in terms of the inter/intra-beam interference, the concurrence time, and the frequency-reuse effectiveness. Finally, section V concludes the paper, highlighting the merits of the PCS's new design and future works.

II. PRINCIPLES OF THE PRIORITY CODE SCHEME

A. DESCRIPTION

In real satellite communication systems, the bandwidth demand of each beam changes from time to time due to the fickle user needs that the beams serve. Therefore, a precise beam might have low bandwidth demand at a particular moment and high bandwidth demand at the next moment. The PCS seeks to increase the bandwidth capacity of beams that shadow specific footprints with a high bandwidth demand. In addition, the PCS seeks to minimize the amount of resources allocated to beams with low bandwidth demands. Based on the PCS algorithm [12], the PCS dynamically increases or reduces the frequency resource allocation by identifying three possible scenarios: the accurate bandwidth allocation, the underload bandwidth allocation and the overload bandwidth allocation. The underload and the overload bandwidth allocations are undesirable occurrences.

To identify undesirable allocation occurrences, the PCS algorithm uses three parameters: the efficiency ratio η_r, the efficiency indicator η_i, and the efficiency threshold η_t. The efficiency ratio η_r represents the ratio of bandwidth utilization to bandwidth capacity at a particular moment. The efficiency ratio η_r changes from time to time in accordance with the bandwidth utilization variations. The efficiency indicator η_i is the efficiency ratio value that indicates when the PCS executes an accurate bandwidth allocation. The efficiency indicator η_i is a constant variable defined in the PCS's initial premises. Therefore, it is fundamental to set it up at the beginning of the PCS algorithm. The efficiency threshold η_t represents a range of efficiency ratio values that tend to be equal to the efficiency indicator value. The efficiency threshold η_t is the result of adding an approximation parameter to the efficiency indicator η_i and contributes to identifying the underload and overload bandwidth allocations. For instance, if the efficiency ratio η_r is inside the range of values of the efficiency threshold η_t, the bandwidth allocation is correct. Otherwise, the bandwidth allocation is underloaded or overloaded.

For an underload bandwidth allocation, the efficiency ratio η_r is bigger than the values within the efficiency threshold η_t. To solve an underload bandwidth allocation, the beam needs to receive additional bandwidth and its priority code must increase. By contrast, an overload bandwidth allocation occurs when the efficiency ratio η_r is smaller than the values within the efficiency threshold η_t. The overload bandwidth allocation takes place every time the beam receives more capacity than it needs. Therefore, to reverse the overload bandwidth allocation, the beam must release part of its bandwidth until its satisfies the current demands of the beam without implicating unused frequency resources.

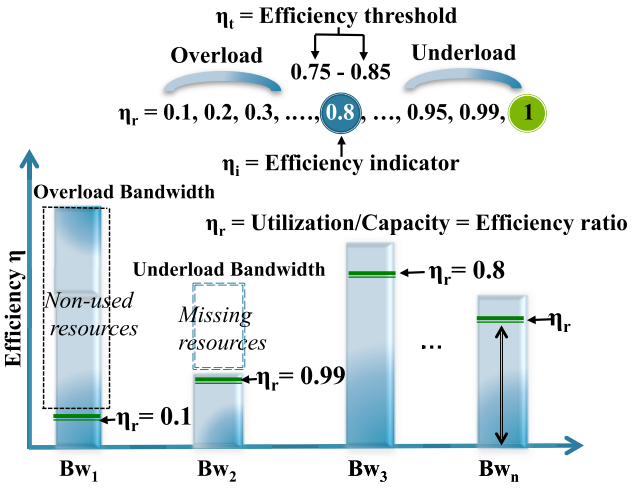

FIGURE 3. Allocation scenarios of the PCS.

The priority code in this scenario decreases in order to match the new bandwidth allocation among the beams. Fig. 3 illustrates the bandwidth allocation scenarios [12] where the efficiency indicator η_i is equal to 0.8 and the approximation parameter is equal to 0.05. Observing Fig. 3, B_{w3} depicts the situation in which the PCS executes an accurate bandwidth allocation. For such scenarios, the PCS does not need to execute a bandwidth adjustment and the priority code remains unchanged. The reason why B_{w3} shows an accurate allocation scenario is that it has an efficiency indicator η_i equal to 0.8, and this value is inside the efficiency threshold η_t defined, that is, equal to 0.8 ± 0.05. In turn, the underload bandwidth allocation is the scenario in which the efficiency ratio η_r approximates to 1 and $\eta_r > 0.85$, for instance the one performed in B_{w2}. By contrast, the overload bandwidth allocation occurs when the efficiency ratio η_r approximates to 0 and $\eta_r < 0.85$, for example, the one executed in B_{w1}. Regarding the priority codes of B_{w1} and B_{w2}, the PCS matches their bandwidth utilization with new priority codes in order to determine which beams require major attention. The bandwidth allocation adjustment is faster in high-demand beams than in low-demand beams. Refer to Fig. 4 to

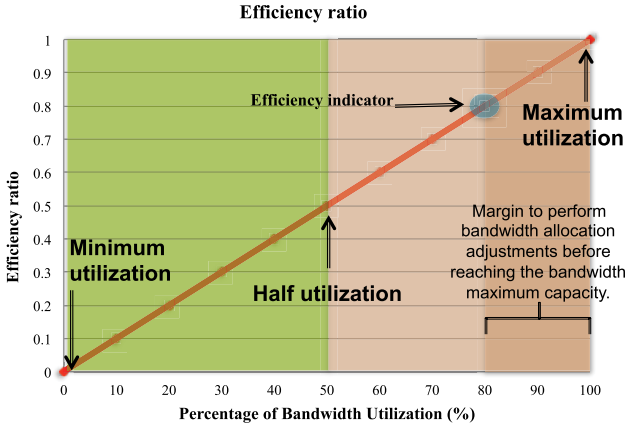

FIGURE 4. Performance of the PCS efficiency ratio.

understand the adequacy offered by an efficiency indicator η_i is equal to 0.8. The most convenient efficiency indicator η_i is the one adjacent to the maximum bandwidth utilization because this ensures a high bandwidth utilization percentage.

Furthermore, the efficiency indicator η_i should be sufficiently distant from the maximum bandwidth utilization. That is because the PCS algorithm requires sufficient time to identify unsuitable bandwidth allocations and to execute the appropriate bandwidth adjustments. In addition, the PCS algorithm must adjust the bandwidth allocation before the beam reaches its maximum bandwidth capacity to avoid the underload bandwidth allocation or before the beam decreases its bandwidth utilization to avoid the overload bandwidth allocation. In conclusion, Fig. 5 illustrates the PCS algorithm, which consists of seven steps.

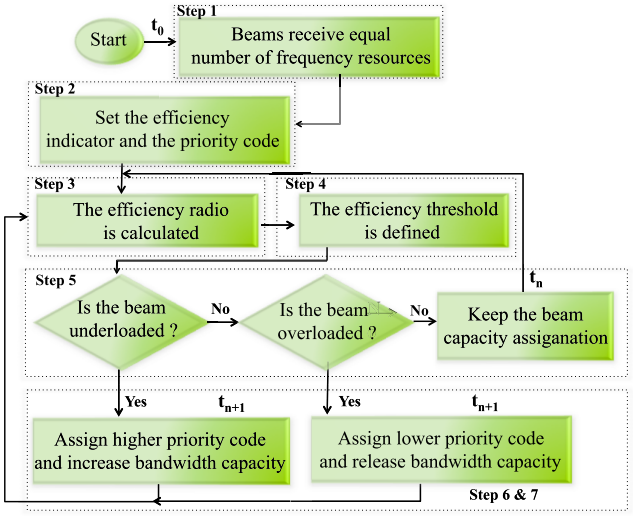

FIGURE 5. Scheduling algorithm of the PCS.

The PCS algorithm initiates assuming all beams receive the same capacity, that is, all beams have a correlative amount of bandwidth. All beams receive an identical priority code as well. That is because, at the beginning of the PCS algorithm, there is no capacity utilization information, nor are there beam efficiency records. The initial priority code corresponds to the given initial bandwidth requirements. Therefore, once the PCS sets the initial bandwidth capacity and the priority code of each beam, the monitoring process starts to operate to obtain the current parameter information related to the bandwidth requirements of each beam in the system.

The information obtained helps to categorize the allocation events under the accurate bandwidth allocation, the underload bandwidth allocation, and the overload bandwidth allocation. The PCS algorithm performs as follows:

- Step 1: The PCS starts. All beams receive the same amount of frequency resources.
- Step 2: The PCS sets an efficiency indicator and a priority code for each beam.
- Step 3: The PCS calculates the efficiency ratio of each beam, dividing the bandwidth utilization by the bandwidth capacity per beam. The PCS learns the bandwidth requirements of the beams by monitoring the efficiency ratio that corresponds to a particular footprint.
- Step 4: The efficiency threshold of each beam is defined based on the efficiency indicator.
- Step 5: The PCS employs the efficiency indicator, the efficiency threshold, and the efficiency ratio to judge which beams have an underload or an overload bandwidth allocation.
- Step 6: The PCS provides a new priority code to each beam that corresponds with the current bandwidth needs by considering the efficiency ratio.
- Step 7: The PCS adjusts the amount of frequency resources assigned to each beam, increasing or decreasing the amount of resources it. Finally, the PCS algorithm cyclically repeats from Step 3 to measure the efficiency ratio of each beam again.

B. INITIAL PERFORMANCE

The evaluation only involves the forward link and uses Ka-band frequencies of the range of 19.6-22.2 GHz. The theoretical scenario refers to 70 beams ($B_{w1}, B_{w2}, \ldots, B_{wn}$) sharing the total bandwidth of 600 MHz, which is divided into blocks of 100 kHz. The authors apply the Shannon's channel coding theorem [13] to analyze the maximum bandwidth capacity of each beam. Equations (2) and (2) define the maximum bandwidth capacity of the beams, where BW represents the bandwidth, $S/(N+I)$ is the signal-to-noise ratio plus interference, P_{TWTA} is the payload on the spacecraft, G_{TX} and G_{RX} are the antenna gain at the transmitter and at the receiver, respectively, d represents the distance between the transmitter and receiver, λ stands for the wavelength, K_B is the Boltzmann's constant, T_{SYST} is the system noise temperature, and I stands for the interference.

$$C = BW\ log_2\left(1 + \frac{S}{N+I}\right) \tag{1}$$

$$\frac{S}{N+I} = \frac{P_{TWTA}\ G_{TX}\ G_{RX}}{\left(\frac{4\pi d}{\lambda}\right)^2 K_B\ T_{SYST}\ BW\ I} \tag{2}$$

Based on the priority codes shown in Table 1, the PCS determines the codes that the beams may adopt based on their efficiency ratio values. In this context, Table 1 includes four codes in which the beam with priority code 4 has the highest importance and the beam with priority code 1 has the lowest importance. Figs. 6 and 7 depict the PCS's initial evaluation results [12].

TABLE 1. Priority codes based on the efficiency ratio.

Demand	Priority Code	Efficiency (%)
High	4	60
Medium	3	25
Low	2	10
Little	1	5

These results represent an average of the tracking performance of the PCS algorithm against the temporal change of

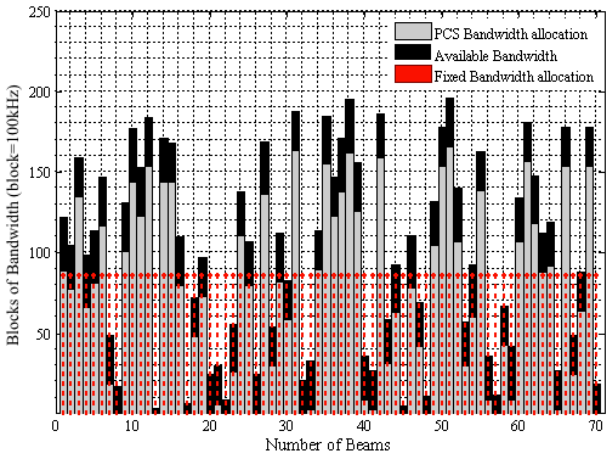

FIGURE 6. PCS employing 70 beams.

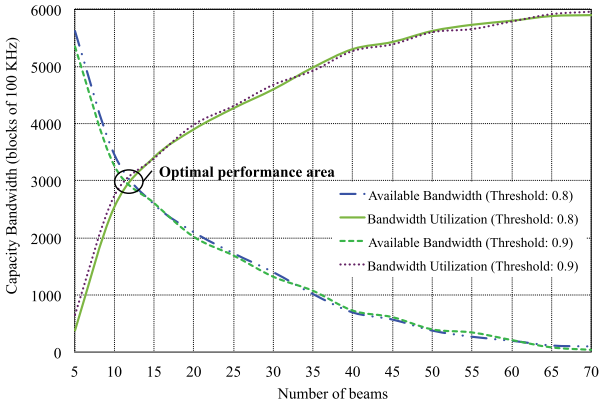

FIGURE 7. PCS capacity for different efficiency thresholds.

the traffic demand based on multiple cases of traffic demand. Fig. 6 considers two types of bandwidth distribution: the fixed bandwidth allocation in which every beam receives a correlative bandwidth capacity and the PCS bandwidth allocation in which the beams receive dynamic bandwidth allocations. The fixed bandwidth allocation does not take care of ongoing user requirements. Consequently, the existence of underload and overload bandwidth allocations, without the opportunity to reverse their effects, is inevitable. Conversely, the PCS bandwidth allocation fairly shares the bandwidth among beams according to the prevailing user needs. In addition, applying the PCS, a beam with $\eta_r > \eta_t$ receives extra bandwidth in comparison to other beams. Beams with $\eta_r < \eta_t$ release bandwidth. At the same time, beams with higher priority codes receive faster assistance from the PCS algorithm than beams with lower priority codes. Fig. 6 shows the scenarios with 70 beams deployed. The dotted line represents the fixed bandwidth allocation case with 8.5 MHz per beam. The bars in gray represent the PCS bandwidth allocation and the bars in black represent the available capacity. Each bar in Fig. 6 corresponds to a particular beam in the system configuration. At first sight, the authors observed that, regardless the number of beams, the PCS avoids the underload and overload scenarios, offering good performances among all beams in the HTS. The PCS proves that it is able to adjust the bandwidth allocation as a function of the number of beams and the fickle bandwidth requirements.

Fig. 7 shows the behavior of the bandwidth utilization against the available bandwidth as a function of the number of beams deployed in the HTS. The corresponding calculations employ different efficiency threshold values ($\eta_t = 0.8, 0.9$) and consider the average of the user's traffic demands by running several iterations. According to Fig. 7, the optimal performance is at 12 beams with contrasted variations from one up to 60 beams. The results also suggest that the PCS might adopt different behaviors by modifying the efficiency threshold values. For instance, if the efficiency threshold decreases, the number of beams of the optimal performance area increases. Conversely, if the efficiency threshold increases, the number of beams of the optimal performance decreases. Therefore, the efficiency threshold value is inversely proportional to the number of beams of the optimal area. In this context, it is remarkable to point that for multi-beam environments it is better to deploy a larger number of beams than a smaller number of beams.

III. PCS's ADDITIONAL CHALLENGES

The PCS succeeds in dynamically allocating bandwidth resources based on user demands in situations in which fixed bandwidth allocations are unsuitable. Consequently, analyzing the concurrence time and the algorithm tardiness is of great relevance. This assumption is based on the fact that the PCS needs to react in an opportunistic way to ensure the reliability of the scheme. Regarding multi-beam environments, it is useful to enhance the frequency resources by sharing these resources among the beams. In this context, the frequency-reuse process involves an additional interference between adjacent beams, that is, intra-beam group interference, and between adjacent beam groups, that is, inter-beam group interference. Therefore, the present section studies these implications. Based on the analysis performed, the authors expect to extend the contributions of PCS.

A. CONCURRENCE TIME AND ALGORITHM TARDINESS

The concurrence time defines how regularly the PCS runs its algorithm with the purpose of monitoring the efficiency ratio of all beams in the system. Hence, it is relevant to point out that the concurrence time benefits from being part of a priority algorithm [14] to manage the existence of conflicts between diverse tasks in progress. When the monitoring process of a $beam_X$ with *priority code X* is still in progress and the monitoring process related to a $beam_Y$ with *priority code Y* is scheduled, the task with the higher priority keeps going and the task with the lower priority is set to a waiting mode until the PCS algorithm becomes available to assist it. Therefore, this type of decision-making process involves a conflict management analysis. The investigation presented in this research includes these kinds of complexities; however, the progress towards the conflict management process is beyond the scope of this manuscript.

Equation (3) [15] represents the expression of the concurrence time where I_j is the number of incoming beams to be scheduled, R_j is the number of remaining beams to be scheduled, D_j is the number of beams already scheduled, and n stands for the total number of beams.

$$CT(t) = \Sigma_{j=1}^{n}\left(\frac{D_j}{n}\right)\left(\frac{R_j + I_j}{R_j}\right) \tag{3}$$

Algorithm tardiness is defined as the speed with which the PCS algorithm monitors the efficiency ratio of all beams and adjusts the bandwidth allocation of the total number of beams that demand the adjustment. In other words, the algorithm tardiness is an indication of how quickly the PCS runs its algorithm, and it is measured in beams per second (beam/s). As soon as the scheduler accomplishes the total number of tasks, the algorithm starts again. The PCS algorithm is a short-term scheduling algorithm. Therefore the algorithm tardiness must be quite fast in order to facilitate the tasks in short waiting times. In order to deduce the algorithm tardiness, it is essential to analyze the PCS similarly to a concurrence real-time system [14]. As a real-time system, the PCS needs to respond to precise external conditions within a specific finite time in which the processes are treated as tasks.

As a concurrence system, the PCS repeatedly runs several tasks. Therefore, PCS effectiveness depends on the correctness of the results and the time within which the PCS executes them. The algorithm tardiness classifies this scheme similarly to an algorithm of the constructive type. A constructive type is suitable for algorithms that start without a schedule and gradually build one by adding a task at a time. In this context, the PCS dispatches bandwidth allocation to beams one by one, and once the PCS concludes the allocations, the remaining beams with the highest priority are processed. Equation (4) [15] defines the algorithm tardiness.

$$T(t) = \left(\frac{R_j + I_j}{R_j}\right) exp\left(\frac{-max\,(D_j - R_j)t}{K_1}\right) exp\left(\frac{S_j}{K_2}\right) \tag{4}$$

Where I_j represents the number of incoming beams to be scheduled, R_j is the number of remaining beams to be scheduled, and D_j is the number of beams already scheduled. The S_j is the average of the setup times of the beams remaining to be scheduled, K_1 is the due related scaling parameter, K_2 represents the setup-time-related scaling parameter, and t is the time in seconds. K_1 and K_2 are dimensionless quantities and are defined as follows:

$$C_{max} = (\,\Sigma_{j=1}^{n} R_j\,) + n\,S_j \tag{5}$$

$$\Gamma = \frac{D_{max} - D_{min}}{C_{max}} \tag{6}$$

$$\tau = 1 - \left(\Sigma_{j=1}^{n}\frac{D_j}{n\,C_{max}}\right) \tag{7}$$

$$K_1 = \{\Gamma < 0.5 : 4.5 + \Gamma\}\,\{\Gamma \geq 0.5 : 6 - 2\Gamma\} \tag{8}$$

$$K_2 = \frac{\tau}{2\sqrt{\delta}} \tag{9}$$

$$\delta = \frac{S_j}{R_j} \tag{10}$$

Where C_{max} represents the maximum due beams to be scheduled, Γ is the due beam range factor, D_{max} stands for the maximum number of the beams already scheduled, D_{min} is the minimum number of the beams already scheduled, τ represents the due date tightness factor, δ stands for the effectiveness factor of the remaining beams to be scheduled, and n is the total number of beams.

B. PCS FREQUENCY-REUSE

Frequency-reuse refers to the repeated use of the same set of frequencies among several beams. It involves a basic principle that establishes that adjacent beams cannot share the same set of frequencies. The frequency-reuse factor is the rate at which the beams use the same set of frequencies, and it is defined as $R = 1/M$, where M stands for the number of sets of frequencies or the number of beams that cannot share the same set of frequencies. Consequently, the frequency-reuse pattern is related to the configuration of beams that follow the frequency-reuse factor.

The PCS frequency-reuse build follows the subsequent statements:

- There are 70 multi-beams deployed in the HTS.
- The beams are grouped into collections of seven beams each to shape 10 beam groups.
- The beam groups use labels, namely, G, B, and P, to distinguish them from others. Besides, adjacent beam groups cannot share the same label.
- Beam groups with different labels do not share the same set of frequencies and beam groups with same label share the same set of frequencies. Therefore, considering the frequency-reuse pattern, the inter-group frequency reuse factor is $R_{inter} = 1/3$.
- In turn, the beams inside the same group are numbered from 1 to 7, and none of them share a subset of frequencies. Thus, the intra-group frequency-reuse factor is $R_{intra} = 1/7$.

Bearing the previous frequency-reuse descriptions in mind, Fig. 8 illustrates the PCS frequency-reuse plan. The PCS uses Ka-band frequencies of the range of 19.6 - 22.2 GHz. Accordingly, the total available bandwidth is 600 MHz, and

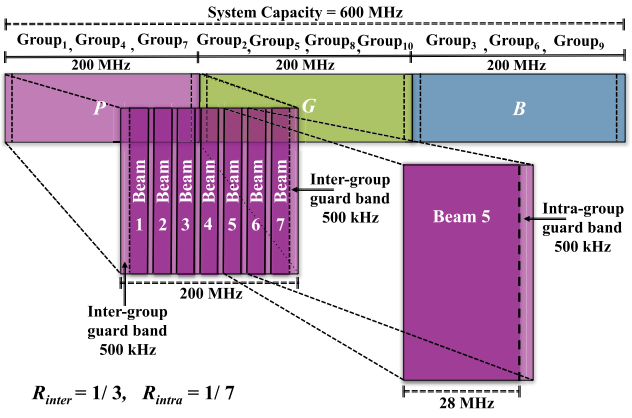

FIGURE 8. PCS Frequency-Reuse Plan.

it is divided to create three sets of frequencies. The PCS frequency-reuse replicates each set every three beam groups. In turn, each set of frequencies is organized into seven subsets of frequencies. Therefore, there is one subset of frequencies for each beam of the group. At the beginning of the algorithm, each set and subset of frequencies is correlatively sized so that each beam group receives a maximum of 200 MHz and each beam receives maximum of 28 MHz, respectively. A remaining bandwidth of 5 MHz is used to form the guard bands of the inter/intra beam groups.

The PCS uses this bandwidth distribution only at the beginning of the algorithm because, after the PCS initialization, the sets of frequencies might be not correlatively sized. After the initialization of the algorithm, the subsets of frequencies might be not correlative either. However, the number of sets and subsets of frequencies and the amount of bandwidth used as guard bands remain without variations to decrease interference among beams. In conclusion, Fig. 9 depicts the scenario of the PCS frequency-reuse plan. Observing Fig. 9, the beams numbered similarly and belonging to beam groups with the same label might have the same subset of frequencies. Following the rules of the frequency-reuse plan, all beams might increase their bandwidth capacity by three times. This evidence is more productive when a PCS beam experiences an underload bandwidth scenario because that scenario is one in which the PCS beam requires extra bandwidth.

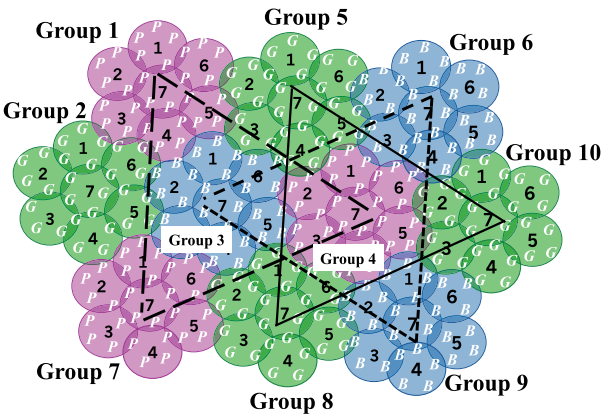

FIGURE 9. HTS Scenario using the PCS Frequency-Reuse Plan.

C. PCS INTERFERENCE

Interference conditions are significant parameters in the quality of service (QoS) of satellite communication systems. The interference conditions might be overwhelmed by: 1) the existence of beams in the same frequency band with overlapping footprints, that is, intra-band interference, and 2) the existence of beams in adjacent frequency bands with overlapping footprints, that is, inter-band interference. The PCS interference model considers 70 multi-beams in an HTS in the GEO orbit. The beam radius B_R is equivalent in all beams, and it is equal to 100 Km. This research involves two types of interference in the PCS. They are intra-group interference and inter-group interference. In turn, both types of interference include intra-band and inter-band interference.

By definition, intra-group interference is interference that affects beams inside the same group. According to the PCS frequency-reuse plan, beams inside the same group use different subsets of frequencies. Therefore, intra-band interference is negligible, resulting in the PCS intra-group interference that only involves the inter-band interference. The PCS interference pattern is based on the presumption that are intra-group guard bands of 500 kHz between beam groups. Fig. 10 represents the PCS intra-group interference model of *Group*1. In Fig. 10 the arrows illustrate the direction of the inter-band interference between adjacent beams belonging to the same group. For instance, $Beam_1$ interferes with $Beam_2$, $Beam_6$, and $Beam_7$. In turn, $Beam_2$ interferes with $Beam_1$, $Beam_3$, and $Beam_7$. $Beam_3$, $Beam_4$, $Beam_5$, and $Beam_6$ follow the same interference behavior. As $Beam_7$ is the only beam that interferes with all beams in the group, it is a unique beam. All beam groups have the same PCS intra-group interference model.

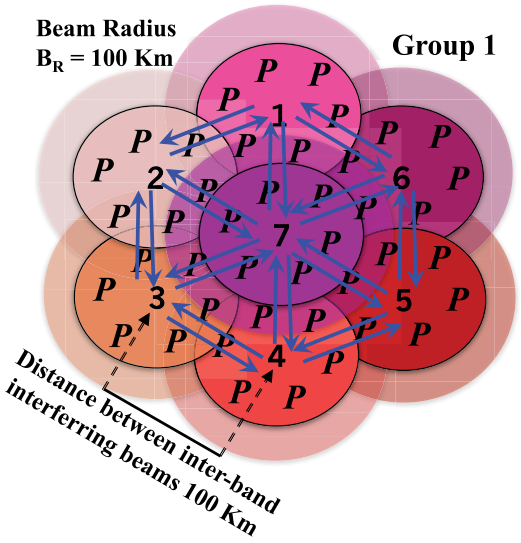

FIGURE 10. PCS intra-group interference model.

The inter-group interference affects beams belonging to different groups. Fig. 11 represents the PCS inter-group interference model in which only four groups, 28 beams, are illustrated. The inter-group interference involves intra-band and inter-band interference as well. Where intra-band interference is concerned, as the interfering beams must share the same subset of frequencies, they must accomplish three conditions: be numbered similarly, belong to different groups, and share the same label (G, B, P). This is because beams in different groups with the same label have the same subset of frequencies and beams in different groups with different labels do not have the same subset of frequencies. For example, observing the dashed arrows in Fig. 11, $Beam_7$ in $Group_1$ only causes intra-band interference with $Beam_7$ in $Group_4$. In turn, $Beam_7$ in $Group_4$ only causes intra-band interference with $Beam_7$ in $Group_1$. $Beam_1$, $Beam_2$, $Beam_3$, $Beam_4$,

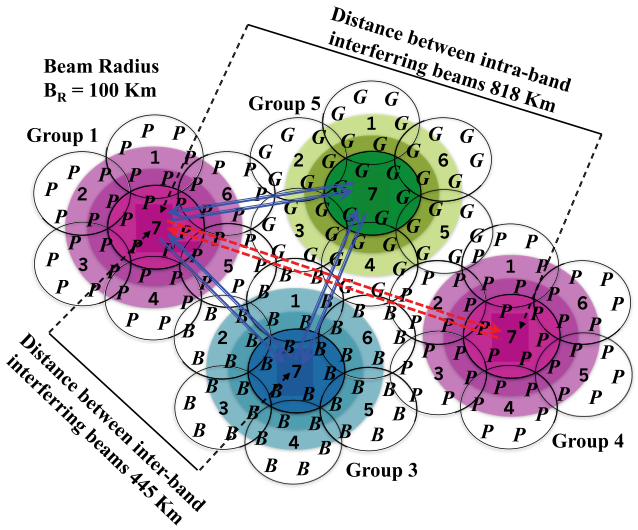

FIGURE 11. PCS inter-group interference model.

$Beam_5$, and $Beam_6$ follow the same intra-band interference performance from $Group_1$ to $Group_{10}$.

Regarding the inter-band interference involved in inter-group interference, the authors observed that the interfering beams must: be numbered similarly, belong to different groups, and have different labels (G, B, P). This is because, based on the PCS frequency-reuse pattern, beams in different groups with different labels have adjacent subsets of frequencies. Accordingly, in Fig. 11, the bold arrows represent inter-band interference. Observing Fig. 11, $Beam_7$ in $Group_1$, $Beam_7$ in $Group_3$, and $Beam_7$ in $Group_5$ cause inter-band interferences among each other. $Beam_1$, $Beam_2$, $Beam_3$, $Beam_4$, $Beam_5$, and $Beam_6$ in $Group_1$ to $Group_{10}$ follow the same inter-band interference performance.

The intra-group interference and inter-group interference are respectively defined in (11) and (12) [16] where Ψ is the inter-band interference that occurs in each group, Υ represents the intra-band interference that occurs between different groups, and Ω stands for the inter-band interference that occurs between different groups. In addition, $EIRP$ is the equivalent isotropically related power, G_r represents the antenna gain of the satellite, L is the free space loss, G_{sh} stands for the shadowing components of the satellite link, BG is the number of beam groups, k represents the number of beams in each group, m is the number of beam groups using adjacent subsets of frequencies, and q stands for the number of beam groups using the same subset of frequencies.

$$I_{intra-group} = \Sigma_{BG=1}^{10} \Psi_{BG} \tag{11}$$

$$I_{inter-group} = \Sigma_{BG=1}^{10} \left(\Upsilon_{BG} + \Omega_{BG} \right) \tag{12}$$

$$\Psi = \Sigma_{k=1}^{7} EIRP_k \, G_{r\,k} \, L_k \, G_{sh\,k} \tag{13}$$

$$\Upsilon = \Sigma_{k=1}^{7} \Sigma_{q=1}^{2} EIRP_{(k,q)} G_{r(k,q)} L_{(k,q)} G_{sh(k,q)} \tag{14}$$

$$\Omega = \Sigma_{k=1}^{7} \Sigma_{m=1}^{4} EIRP_{(k,m)} G_{r(k,m)} L_{(k,m)} G_{sh(k,m)} \tag{15}$$

IV. ANALYSIS AND EVALUATION

In order to evaluate the PCS, the analysis employs 70 multi-beams with fickle bandwidth requirements. Table 1 describes the priority codes used. The prediction of the concurrence time involves 3,600 iterations with the duration of one second for each iteration. Observing Fig. 12, the authors determined that the concurrence time might fall under two types of values, that is short and long values. The authors considered the concurrence time short if it fell into the range of 0 to 0.05 s. If the concurrence time was up to 0.18 s, they considered it long. Furthermore, most long values are approaching 0.08 s, whereas most short values approximate to 0.01 s. Based on Fig. 12, the authors concluded that the concurrence time might adopt different behaviors. For instance, if there were many bandwidth adjustments, the concurrence time was short and the PCS algorithm ran rapidly. Conversely, if there were few bandwidth adjustments, the concurrence time was long and the PCS algorithm ran slowly. In conclusion, the docility of the concurrence time proves that the PCS algorithm is flexible and, as a consequence, the PCS responds to dynamic bandwidth demands.

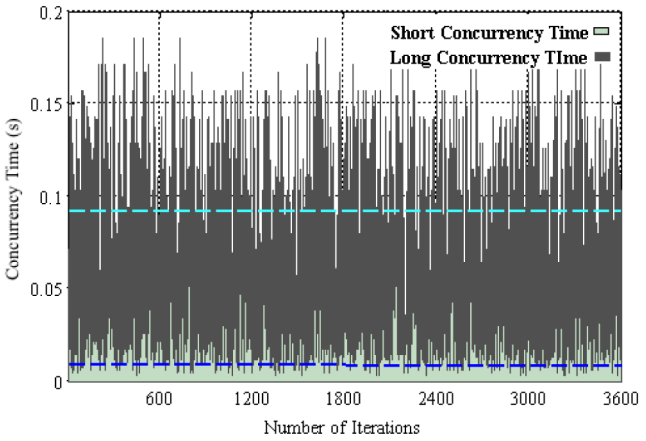

FIGURE 12. Performance of the PCS concurrence time.

In terms of algorithm tardiness, the present analysis attempts three consecutive events. Thus, Fig. 13 depicts these events as follows: Fig. 13.a represents $Event_1$ from 0 to 60 s, Fig. 13.b shows $Event_2$ from 60 to 120 s, and Fig. 13.c illustrates $Event_3$ from 120 to 180 s. Each event reflects the average behavior of 70 beams with dynamic bandwidth requirements. Fig. 13 shows that the algorithm tardiness follows unstable patterns among events. The authors expected this result because the hypothetical scenario considered all beams to have different bandwidth requirements from time to time resulting in modifications of the algorithm tardiness. According to Fig. 13, the longest algorithm tardiness falls in the range of 0 to 30 s, that is, $Event_1$.

This is because, before the algorithm initialization occurs, all beams receive correlative bandwidths. Therefore, once the PCS algorithm begins, all beams suffer a vast number of bandwidth adjustments to match the bandwidth capacity

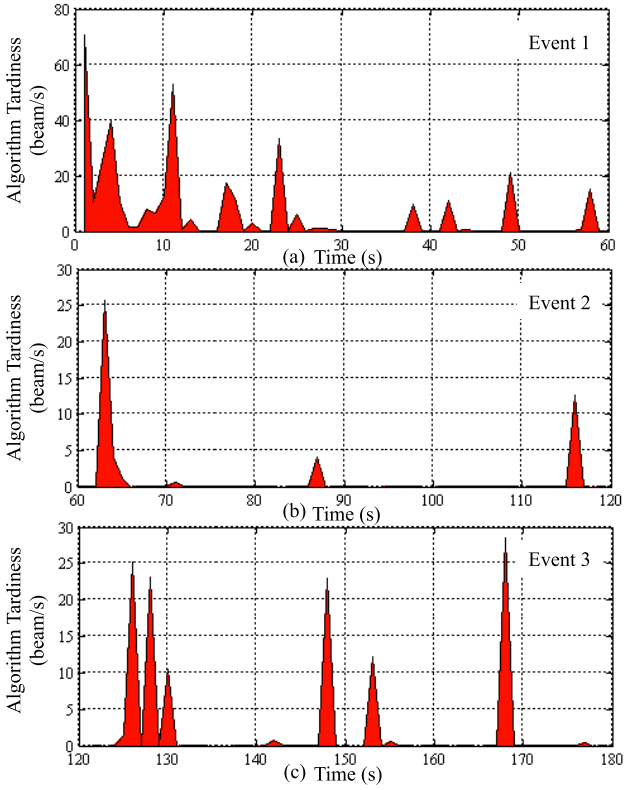

FIGURE 13. Performance of the PCS algorithm Tardiness. Fig. 13.a illustrates the performance of the algorithm tardiness tested from 0 to 60 s, that is Event 1. Fig. 13.b shows the performance of the algorithm tardiness tested from 60 to 120 s, that is Event 2. Fig. 13.c represents the performance of the algorithm tardiness tested from 120 to 180 s, that is Event 3.

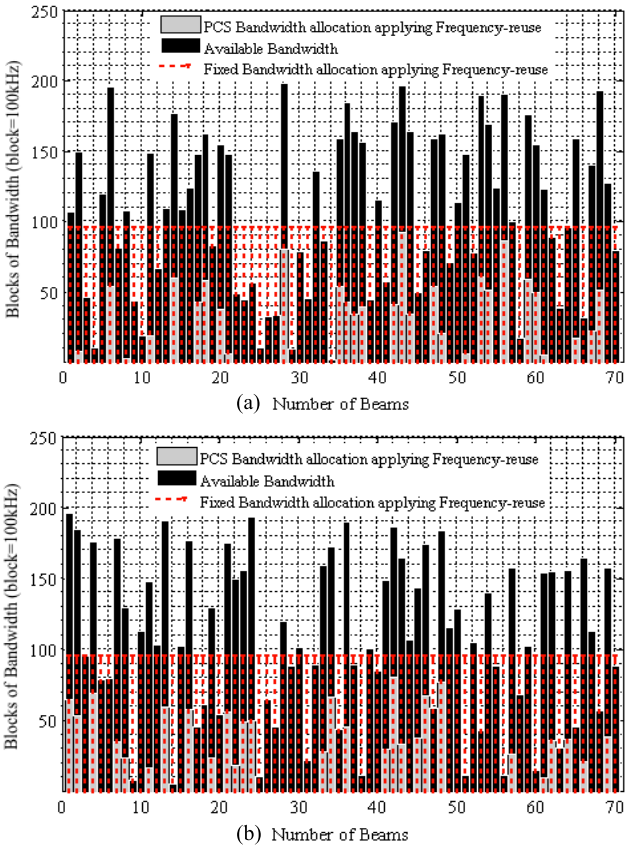

FIGURE 14. Performance of the PCS Employing Frequency-Reuse.

with the current bandwidth requirements. As a consequence, the algorithm tardiness is long at the beginning of the algorithm.

The algorithm tardiness is short if the beams experience few bandwidth modifications, for example, the algorithm tardiness of $Event_2$ from 90 to 120 s. The frames of Figs. 13.b and 13.c suggest that, after the PCS algorithm initializes, the PCS becomes passive and the algorithm tardiness is short. Comparing $Event_1$, $Event_2$, and $Event_3$, the longest algorithm tardiness is equal to 70 beam/s. This is evidence that the monitoring course and the bandwidth adjustment process of each beam need to be performed within 0.014 s. Therefore, the PCS requires a fast algorithm. The shortest algorithm tardiness is approximately 1 beam/s. This means that the monitoring course and the bandwidth adjustment process should be performed in 1 s. Thus, the PCS needs a slow algorithm. The difference between those two values of algorithm tardiness shows that the PCS algorithm has contradictory behaviors.

To complete the PCS evaluation, the authors also analyzed the PCS, presuming that this scheme used the frequency-reuse pattern previously described. The analysis involved 70 multi-beams deployed on an HTS with frequency-reuse factors $R_{inter} = 1/3$ and $R_{intra} = 1/7$. Fig. 14.a illustrates the PCS performance at $t_1 = 60$ s, whereas Fig. 14.b shows the PCS performance at $t_2 = 180$ s. As Fig. 14 illustrates, the performance of the PCS bandwidth allocation applying the frequency-reuse process is more promising than that of the fixed bandwidth allocation applying the frequency-reuse process. The fixed bandwidth allocation represented by the dotted lines, suggests that disregarding the time and the bandwidth demands, the bandwidth allocation of all beams is correlative.

By contrast, the PCS assigns a particular capacity to each beam, and this bandwidth allocation might change from time to time in accordance with the user's bandwidth requirements. The PCS bandwidth allocation performance without the reuse of frequency resources, (which is shown in Fig. 6) is different from the PCS bandwidth allocation with frequency-reuse, (which is shown in Fig. 14), because the total available bandwidth in the first scenario is shared among the total number of beams in the system. In the second scenario, the HTS extends the availability of frequency resources because the total bandwidth is divided by a smaller collection of beams, and this pattern is repeated several times to cover the total number of beams in the system. Generally speaking, the beams that are scheduled by the PCS frequency-reuse extend their bandwidth capacity. Based on the frequency-reuse pattern previously described, the evaluation results suggest that the bandwidth capacity is extended thrice.

TABLE 2. PCS Interference Parameters.

Parameter	Symbol	Value (units)
Effective Isotropically Radiated Power	*EIRP*	60.734 (dB)
Free Space Loss	*L*	208.52 (dB)
Antenna Gain	G_r	119.5 (dBm)
Shadowing Components	G_{sh}	110 - 140 (dBm)

Regarding the PCS interference, the authors assume that the satellite deploys horn antennas with high directivity (20 dB) to increase the directivity of multi-beams. Table 2 recaps some parameters to calculate the intra-band and inter-band interferences. Fig. 15 depicts the results of the PCS interference evaluation. Based on the results provided, the existence of high interference levels in environments that involve the PCS frequency-resource pattern is inevitable. Due to the large number of adjacent beams within HTS systems, the authors expected these results. In conclusion, the interference performance compromises the effectiveness of the PCS.

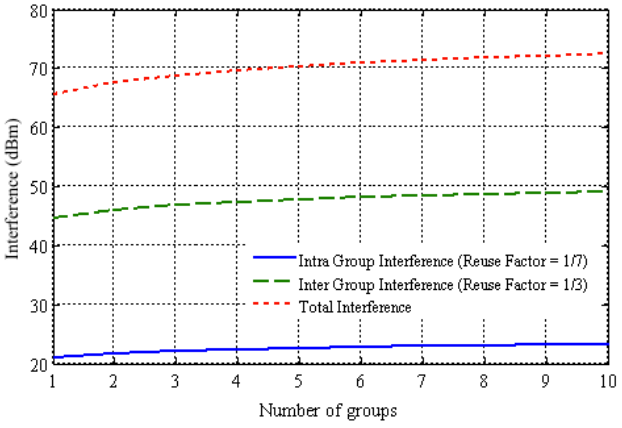

FIGURE 15. PCS Interference Evaluation.

V. CONCLUSION

The present manuscript proved that the PCS algorithm succeeded in dynamically allocating bandwidth resources, based on user demands. This merit is remarkable because, in ongoing situations, the capacity needs of the network follow unstable patterns. The results confirmed that, by applying the frequency-reuse process, the PCS also successfully deals with the scheme's purpose. Furthermore, the PCS frequency-reuse pattern helps to increase the dynamism and the efficiency of the bandwidth utilization. On the other hand, the frequency-reuse process compromises the interference performance within the HTS. Therefore, the frequency-reuse process compensates for the interference with increments in the utilization of frequency resources. Moreover, the results showed that the efficiency threshold values are greater determinants for configurations with fewer beams than for configurations with a larger number of beams. Considering the concurrence time and the algorithm tardiness, the results proved that the PCS succeeded in reflecting the user habits in time and manner by increasing or decreasing the bandwidths previously assigned. The concurrence time and the algorithm tardiness are related to each other: The concurrence time tends to two types of values, which are suitable in case of a small or large number of bandwidth adjustments. The algorithm tardiness also possesses two types of values. In order to qualify the PCS in terms of throughput, future works will be devoted to comparing the PCS with other techniques, such as beam hopping.

REFERENCES

[1] H. Fenech, A. Tomatis, S. Amos, and V. Soumpholphkakdy, "KA-SAT and future HTS systems," presented at the 14th Int. Conf. Vac. Electron., Paris, France, May 2013, pp. 1–2.

[2] O. Vidal, G. Verelst, J. Lacan, E. Alberty, J. Radzik, and M. Bousquet, "Next generation high throughput satellite system," presented at the IEEE 1st AESS Eur. Conf. Satellite Telecommun., Rome, Italy, Oct. 2012, pp. 1–7.

[3] D. Serrano-Velarde, E. Lance, H. Fenech, and G. Rodriguez-Guisantes, "Novel dimensioning method for high-throughput satellites: Forward link," *IEEE Trans. Aerosp. Electron. Syst.*, vol. 50, no. 3, pp. 2146–2163, Jul. 2014.

[4] H. Fenech, S. Amos, A. Tomatis, and V. Soumpholphakdy, "High throughput satellite systems: An analytical approach," *IEEE Trans. Aerosp. Electron. Syst.*, vol. 51, no. 1, pp. 192–202, Jan. 2015.

[5] A. Kyrgiazos, B. G. Evans, and P. Thompson, "On the gateway diversity for high throughput broadband satellite systems," *IEEE Trans. Wireless Commun.*, vol. 13, no. 10, pp. 5411–5426, Oct. 2014.

[6] P. Inigo *et al.*, "Review of terabit/s satellite, the next generation of HTS systems," presented at the 7th Conf. Adv. Satellite Multimedia Syst., 13th Int. Workshop Signal Process. Space Commun., Livorno, Italy, Sep. 2014, pp. 318–322.

[7] J. Anzalchi *et al.*, "Beam hopping in multi-beam broadband satellite systems: System simulation and performance comparison with non-hopped systems," presented at the 5th Conf. Adv. Satellite Multimedia Syst., 11th Int. Workshop Signal Process. Space Commun., Cagliari, Italy, Sep. 2010, pp. 248–255.

[8] T. Pecorella, R. Fantacci, C. Lasagni, L. Rosati, and P. Todorova, "Study and implementation of switching and beam-hopping techniques in satellites with on board processing," presented at the Int. Workshop Satellite Space Commun., Salzburg, Austria, Sep. 2007, pp. 206–210.

[9] K. Kiatmanaroj, C. Artigues, L. Houssin, and F. Messine, "Frequency allocation in a SDMA satellite communication system with beam moving," presented at the Int. Conf. Commun. (ICC), Ottawa, ON, Canada, Jun. 2012, pp. 3265–3269.

[10] L. Yang, Y. Zhang, X. Li, and X. Gao, "Radio resource allocation for wideband GEO satellite mobile communication system," presented at the Int. Conf. Wireless Commun. Signal Process. (WCSP), Hangzhou, China, Oct. 2013, pp. 1–5.

[11] T. Aman, T. Yamazato, and M. Katayama, "Traffic prediction scheme for resource assignment of satellite/terrestrial frequency sharing mobile communication system," presented at the Int. Workshop Satellite Space Commun. (IWSSC), Tuscany, Italy, Sep. 2009, pp. 40–44.

[12] L. H. R. Gaytan, J. Liu, and S. Shimamoto, "Priority code scheme for flexible scheduling in HTS," presented at the IEIE-IEEE Int. Conf. Electron., Inf. Commun., Singapore, Jan. 2015.

[13] H. Fenech, A. Tomatis, S. Amos, V. Soumpholphakdy, and D. Serrano-Velarde, "Future high throughput satellite systems," presented at the IEEE 1st Conf. Aerosp. Electron. Syst. Soc. Eur. Satellite Telecommun., Rome, Italy, Oct. 2012, pp. 1–7.

[14] J. R. Haritsa, M. J. Carey, and M. Livny, "Dynamic real-time optimistic concurrency control," presented at the 11th Real-Time Syst. Symp., Lake Buena Vista, FL, USA, Dec. 1990, pp. 94–103.

[15] M. L. Pinedo, *Scheduling: Theory, Algorithms, and Systems* (Springer Science and Business Media), 3rd ed. New York, NY, USA: Springer-Verlag, 2008, pp. 35–61.

[16] V. Deslandes, J. Tronc, and A.-L. Beylot, "Analysis of interference issues in integrated satellite and terrestrial mobile systems," presented at the 5th Conf. Adv. Satellite Multimedia Syst., 11th Workshop Signal Process. Space Commun., Cagliari, Italy, Sep. 2010, pp. 256–261.

LILIAN DEL CONSUELO HERNANDEZ RUIZ GAYTAN received the B.S. degree in telecommunications from the Engineering Faculty, National Autonomous University of Mexico, in 2004, and the M.S. degree in engineering and science from the Graduated School of Global Information and Telecommunication Studies, Waseda University, Japan, in 2012, where she is currently pursuing the Ph.D. degree. From 2004 to 2006, she was with Panasonic Corporation, Mexico. From 2006 to 2009, she was with Telcel as a member of the Radio Frequency RAN Engineer team. From 2013 to 2014, she was invited by Ericsson Mexico to work as an RAN Consultant in USA. Her research interests are satellite communications, mobile communications, and cloud networks.

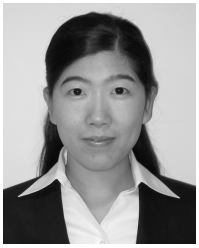

ZHENNI PAN received the B.S. degree in computer science engineering from China Agricultural University, China, in 2007, and the M.S. degree in information and telecommunications from the Graduate School of Global Information and Telecommunication Studies, Waseda University, Japan, in 2011, where she is currently pursuing the Ph.D. degree. She has been a Research Associate with Waseda University since 2013. Her research interests include green wireless communications, heterogeneous cellular networks, intelligent transportation systems, and optical communication.

JIANG LIU received the B.S. degree in electronics engineering from the Chongqing University of Technology, China, in 2001, and the M.S. and Ph.D. degrees in information and telecommunications from the Graduate School of Global Information and Telecommunication Studies, Waseda University, Japan, in 2006 and 2012, respectively. She was a Research Associate with Waseda University from 2009 to 2012. She is currently an Assistant Professor with the International Center for Science and Engineering Programs, Faculty of Science and Engineering, Waseda University. Her research interests include optical wireless communications, intelligent transportation systems, and wireless network security.

SHIGERU SHIMAMOTO received the B.E. and M.E. degrees from the University of Electro Communications, Tokyo, Japan, in 1985 and 1987, respectively, and the Ph.D. degree from Tohoku University, Sendai, Japan, in 1992. He was with NEC Corporation from 1987 to 1991. From 1991 to 1992, he was a Research Associate with the University of Electro Communications. He was a Research Associate with Gunma University, Gunma, Japan, from 1992 to 1993. From 1994 to 2000, he was an Associate Professor with the Graduate School of Global Information and Telecommunication Studies (GITS), Waseda University, Tokyo. He was a Visiting Professor of Electrical Engineering with Stanford University in 2008. Since 2001, he has been a Professor with the Department of Communications and Computer Engineering, GITS, Waseda University. He is currently the Associate Dean of GITS, and a Professor with the Department of Communications and Computer Engineering, Waseda University. His main fields of research include satellite communications, mobile communications, optical wireless communications, ad-hoc networks, sensor networks, and body area networks.